J Mol Model (2011) 17:1735–1741
DOI 10.1007/s00894-010-0875-5

ORIGINAL PAPER

Flexibility of the exportins Cse1p and Xpot depicted by elastic network model

Mingwen Hu · Byung Kim

Received: 21 July 2010 / Accepted: 8 October 2010 / Published online: 7 November 2010

Abstract Nucleocytoplasmic transport in eukaryotic cells involves many interactions between macromolecules, and has been an active area for many researchers. However, the precise mechanism still evades us and more efforts are needed to better understand it. In this study, the authors investigated exportins (Cse1p and Xpot) by elastic network interpolation (ENI) and elastic network based normal mode analysis (EN-NMA). Results of the study on Cse1p were in good agreement with the results obtained by molecular dynamics simulation in another study but with the benefit of time-efficiency. First, a formation of ring closure obtained by ENI was observed. Second, HEAT 1 to 3 and HEAT 14 to 17 had the largest values of root mean square deviation (RMSD) which indicated the flexibility of Cse1p during the transition. In the case of Xpot, a possible pathway from nuclear state to cytoplasmic state was shown, and the predicted pathway was also quantitatively analyzed in terms of RMSD. The results suggested two flexible regions of Xpot that might be important to the transporting mechanism. Moreover, the dominant mode of Xpot in the nuclear state obtained by EN-NMA not only showed the tendency to match the predicted pathway to the cytoplasmic state of Xpot, but also displayed the flexible regions of Xpot. A time-efficient computational approach was presented in this paper and the results indicated that the flexibility of tested exportins might be required to perform the biological function of transporting cargos.

Keywords Elastic network model · Exportin · Karyopherin · Nucleocytoplasmic transport

Electronic supplementary material The online version of this article (doi:10.1007/s00894-010-0875-5) contains supplementary material, which is available to authorized users.

M. Hu · B. Kim
Mechanical and Industrial Engineering,
University of Massachusetts,
Amherst, MA 01003, USA

B. Kim (✉)
ELAB 301, 160 Governors Dr,
Amherst, MA 01003, USA
e-mail: kim@ecs.umass.edu

Introduction

The study of nucleocytoplasmic transport in eukaryotic cells has been a very active area for many researchers [1–8], because it involves sophisticated interactions of macromolecules such as spatial separation, dislocation and recognition. The nucleocytoplasmic process between cytoplasm and nucleus is performed by transport factors which carry their cargos and pass through nuclear pore complexes (NPCs) selectively. Most of transport factors belong to the family of β-karyopherin proteins [7, 8]. This type of proteins is built from a tandem series of HEAT repeats and each HEAT unit consists of two antiparallel α helices linked by a turn [4]. Within this family, a transport factor that moves cargo proteins from the cytoplasm into the nucleus is called importin and one that transports in the opposite direction is called exportin. In cytoplasm, importins interact with cargo proteins directly or indirectly by adaptor proteins and then release cargos in the nucleus [6, 8]. A schematic figure of this cycle is shown in Fig. 1 [8]. In the process of releasing cargos, RanGTP plays a

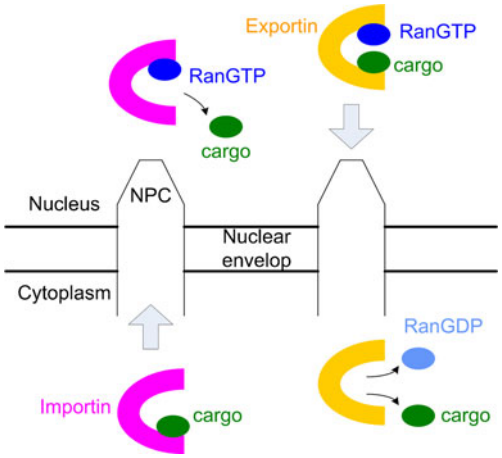

Fig. 1 Schematic representation of nuclear transport between nucleus and cytoplasm [8]

significant role by binding with importins and dissociating the complex of importins. In the case of transport of exportins, the cargo complex is dissociated in the cytoplasm due to GTP hydrolysis. The β-karyopherin proteins have been well studied, however, the precise mechanism still evades us and more efforts are needed to better understand it. In this paper, a time-efficient approach for studying the flexibility of exportins is presented which may provide different perspectives into intriguing interaction of macromolecules within the transport cycle at a low computational cost. Two exportins (Cse1p and Xpot) were chosen for this study because their X-ray structures have been identified, and they have distinct conformational changes in the nucleus and the cytoplasm.

Methods

Elastic network model based interpolation [9] (ENI) was used to study the mechanism of exportins (Cse1p and Xpot). The key principle of ENI is to evenly interpolate the distance between two known conformations of a macromolecule within the context of the elastic network model, a model defined by a macromolecule's structure in terms of point masses and springs [10]. By applying ENI, a possible pathway with 99 intermediates are generated to represent the transition of a target macromolecule regarding its conformational change [9]. Furthermore, elastic network based normal mode analysis (EN-NMA) was also applied to exportin-t (Xpot). EN-NMA is a harmonic fluctuation of a molecule around its equilibrium state within an elastic network [11–13]. Details of the mathematical derivation of ENI and EN-NMA can be found elsewhere [9, 14]. In this study, only alpha carbons of exportins were taken into account and a cutoff distance of 12 angstroms was used in the elastic network models. All calculations were carried out in MATLAB.

Results and discussion

Cse1p

Importin-α,β/CAS system has attracted many researcher's attention among all nuclear transports because it is relatively less complicated and many structures of components within the cycle have been determined [4, 6, 7]. In this classical system, the transport factor CAS (Cse1p in yeast [15, 16]) carries cargos (importin-α) across NPCs and the complex of cargos and CAS is dissociated by RanGTP hydrolysis in the cytoplasm. Upon this transport, Cse1p undergoes a distinct conformational change to perform the biological functions of carrying and releasing cargos in eukaryotic cells.

In order to obtain a possible transition of a chosen macromolecule upon conformational change, two coordinates of terminals are required for the calculation of ENI. In the case of Cse1p, the starting position was the conformation (open form) in the nuclear state (PDB: 1WA5 [17]) and the ending position was the conformation (closed form) in the cytoplasmic state (PDB: 1Z3H [18]). In the form of cargo-binding state (1WA5), two binding sites of RanGTP are recognized at Heat 1-3 and Heat 13-14 together with Heat 19. On the other hand, the binding sites of Kap60p are outer surface of Heat 5-7, Heat 2-4, and Heat 19. All these sites of Cse1p are highly relevant to its biological function of cargo transport.

The goal of performing ENI was to obtain a possible pathway for the conformational change of Cse1p, so the corresponding atoms in two states should be identical. Consequentially, coordinates of Kap60p cargos and RanGTP in 1WA5 were removed and only residues which exist in both states were taken into account for the simulation. Finally, a possible pathway with a series of intermediates (i.e., 99 intermediates) was obtained and displayed in Fig. 2 (Movie S1 in the Supplementary materials).

In Zachariae's study [19], the authors performed a 10 ns molecular dynamics (MD) simulation at 1WA5, the form in the nuclear state, and then obtained a final structure at the end of simulation which was very close to the structure of 1Z3H, the form in the cytoplasmic state. In addition, they also observed and displayed the movement of ring closure from the 10 ns-transition. From our simulation, the results were in good agreement with Zachariae's work. First, the movement of ring closure was observed in the result of ENI as well (Fig. 2). Second, the authors calculated the average

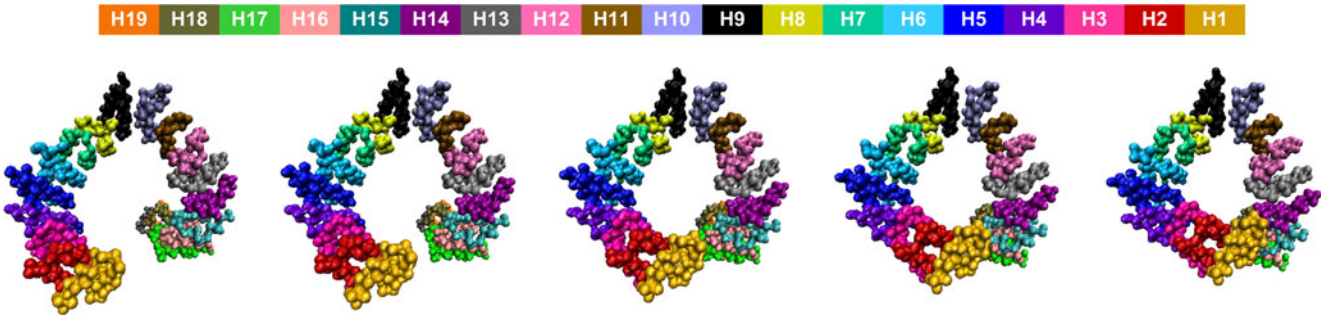

Fig. 2 A possible pathway of Cse1p regarding the conformation change from nuclear state to cytoplasmic state (Left to Right). All figures of intermediates were generated by VMD [31]

of RMSD with respect to every 20 Heat during this conformational change from open (1WA5) to closed form (1Z3H). The average of RMSD for each Heat was calculated by Eq. 1 and was shown in Fig. 3.

$$Heat(i)_{average} = \frac{1}{98}\left(\sum_{j=1}^{98} RMSD(j_{th}, j_{th+1})\right) \quad (1)$$

where $RMSD(j_{th}, j_{th+1})$ represents the value of Root Mean Square Deviation (RMSD) between j_{th} intermediate and j_{th+1} intermediate which are generated by ENI, i is the index of each Heat (i is 20 in the case of Cse1p). This value could be a quantitative index to characterize each intermediate during the transition. In addition, a profile of how RMSD of each Heat varied during the transition was provided in Fig. S1 in Supplementary materials.

The result of Fig. 3 shows that Heat 1-3 and Heat 14-17 have the largest values of average RMSD, and Heat 7-10 have the least values of average RMSD. These observations were similar to the results reported in Zachariae's work. The above results suggest that our simulation of ENI has a capability similar to the MD simulation in predicting the

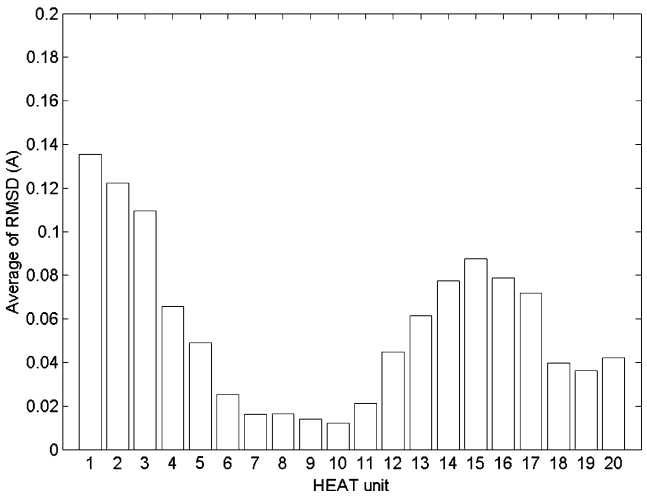

Fig. 3 Average of RMSD of Cse1p's 20 HEAT units during the transition predicted by ENI from nuclear state to cytoplasmic state

flexibility of nuclear transport on exportins in terms of displaying a series of intermediates and RMSD but uses much less computational time. However, this computational method has one limitation in that coordinates of two end conformations are required for generating a possible pathway. On the other hand, only one known conformation is needed for starting a MD simulation as in Zachariae's work. In our simulation of Cse1p, the computational time for obtaining all 99 intermediates by ENI was about 3 hours and 50 minutes on an Intel-Xeon 3.2 GHz 16 GB Ram PC.

Xpot

It is well-known that the transport of RNA between the nucleus and cytoplasm is a key process for gene expression [20, 21]. In the case of tRNA, it is loaded by the transport factor protein exportin-t (Xpot) in the nucleus (i.e., the site where the transcription takes place) and transported to the cytoplasm (i.e. the site where the translation takes place) by passing through the NPCs [20]. Like other routes of nuclear exports, RanGTP highly participates in this process. tRNA binds to Xpot with RanGTP in the nucleus and releases tRNA by hydrolysis of RanGTP in the cytoplasm [21]. Xpot is also a member of β-karyopherin proteins ,and both X-ray structures in cytoplasmic and nuclear states (3ICQ and 3IBV) were recently reported [22]. Similar to other β-karyopherin families, it has 19 tandems of HEAT which comprises two antiparallel α helices for each repeat. In general, Xpot's structure can be described as a complex of two arches, N-terminal arch (Heat 1 to Heat 9) and C-terminal arch (Heat 10 to Heat 19). In the state of binding RanGTP and tRNA (3ICQ: the nuclear state), three components highly interact to each other. Most interactions between RanGTP and Xpot are located at N-terminal arch which includes Heat 1-4 and Heat 9. Other regions of interaction are located at Heat 13 and Heat 17 of C-terminal arch. As to the interactions between tRNA and Xpot, tRNA is enclosed by some regions of Xpot. For example, the acceptor arm of tRNA binds at the surface of Heat 8-18 of

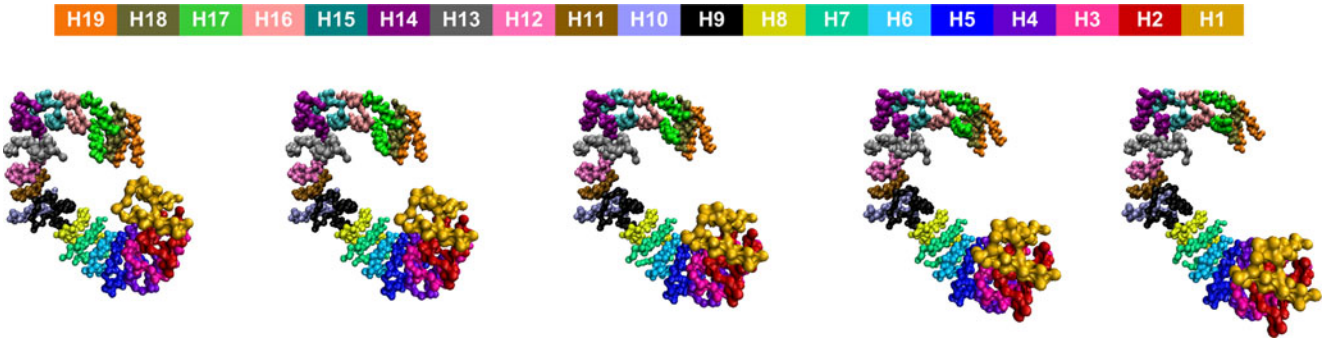

Fig. 4 A possible pathway of Xpot regarding the conformation change from nuclear state to cytoplasmic state (Left to Right). All figures of intermediates were generated by VMD [31]

Xpot. More detailed structural analysis can be found in Cook's work [22].

Prior to the simulation of ENI, coordinates of RanGTP and tRNA were removed from 3ICQ, the conformation in the nuclear state, to coincide with the coordinates of 3IBV, the conformation in the cytoplasmic state. Finally, a possible pathway with a series of intermediates was obtained and displayed in Fig. 4 (Movie S2 in the Supplementary materials). Additional two movie clips (Movie S3 and S4) with different orientations then Movie S2 were also provided as Supplementary materials. The authors encourage readers to watch the Supplementary material Movie S2–S4 for better observation of the predicted dynamic transition. In generating all 99 intermediates between 3ICQ and 3IBV, it took computational time of 2 hours and 20 minutes on an Intel-Xeon 2.33 GHz 64 GB Ram PC. To the author's best knowledge, this is the first report of displaying transition regarding Xpot's conformational change.

The series of intermediates in Fig. 4 represents the movement of ring opening which is opposite to the ring closure observed in Cse1p. It might be helpful to understand how Xpot performs releasing cargos by a stepwise fashion of pathway. According to Fig. 4 and Movie S2, the major dynamic movements could roughly recognized by two parts, Heat 1-5 and Heat 13-19. The first part is rotating down to the bottom, and its orientation is clearer in Movie S4 which shows a clockwise rotation. On the other part (Heat 13-19), it is rising and rotating up to the top. In other words, these two parts of Xpot were very flexible during this conformational change. Moreover, this dynamic transition was analyzed quantitatively in terms of values of average RMSD as shown in Fig. 5. In Fig. 5, the average of RMSD was calculated based on Eq. 1 (i is 19 in the case of Xpot) during the predicted transition from bound state (3ICQ) to unbound state (3IBV). The result of Fig. 5 shows that Heat 1-4 of N-terminal arch and Heat 16-19 of C-terminal arch had larger displacements during this cargo-induced conformational change. In addition, a profile of how each HEAT varied during the transition in terms of average RMSD was shown in Fig. 6. It shows that all Heat repeats displayed an interesting pattern that there were two

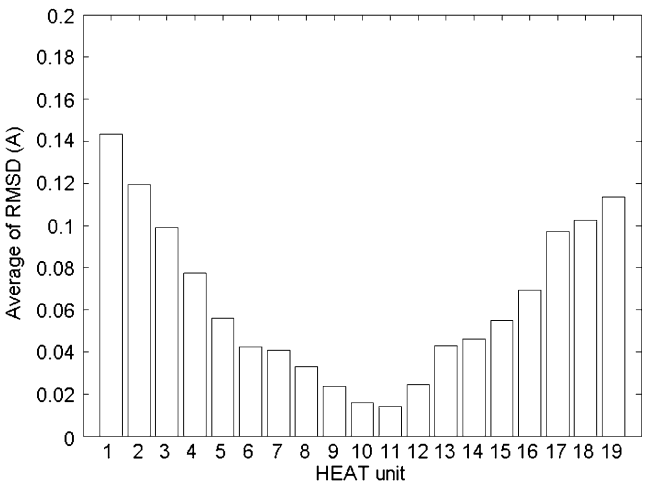

Fig. 5 Average of RMSD of Xpot's 19 HEAT units during the transition predicted by ENI from nuclear state to cytoplasmic state

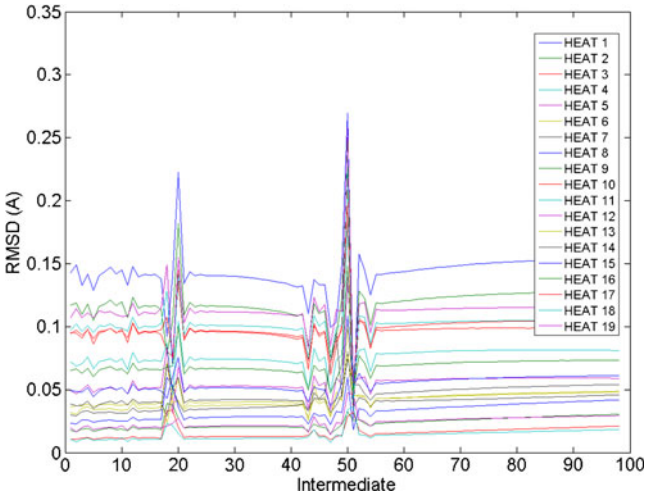

Fig. 6 The profile of how each HEAT of Xpot changed during the transition predicted by ENI

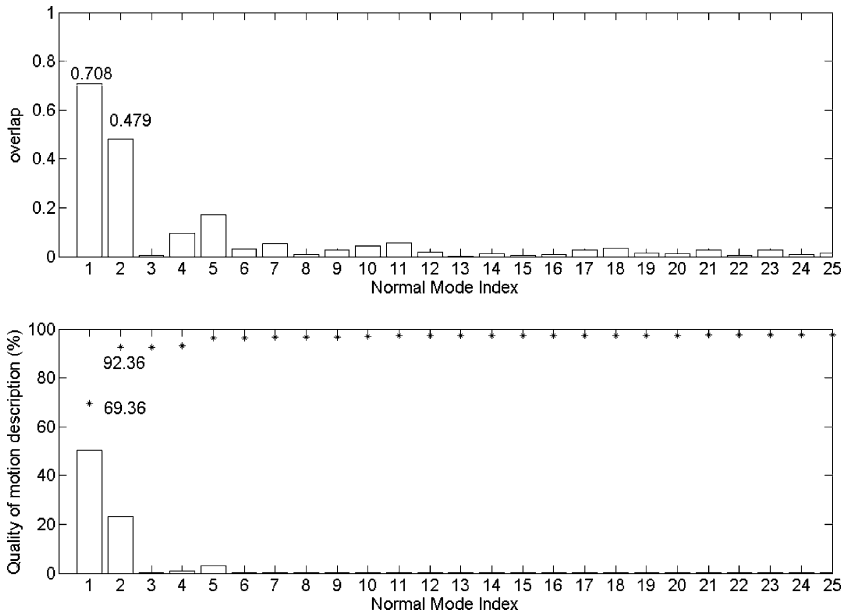

Fig. 7 The plot of values of overlap (Top) and quality of motion description (Bottom)

distinct increases of average RMSD around 20th and 50th intermediates. In other words, each Heat repeat was sequentially subjected to two major molecular displacements during the transition. Although the authors did not find significant variances such as new contacts or rearrangements between Heat repeats in these intermediates, it is still surprising that each Heat repeat experiences such similar pattern in atomic level.

All above results suggest that Heat 1-4 of N-terminal arch and Heat 16-19 of C-terminal arch were the most flexible regions of Xpot during the predicted dynamic transition. This signature might be crucial in order to release tRNA and RanGTP during the nuclear transportation. In the bound state of Xpot, RanGTP is mainly wrapped by Xpot which includes Heat 1-4 of N-terminal arch, Heat 9, Heat 13 and Heat 17 of C-terminal arch. According to the predicted pathway, Heat 1-4 of N-terminal and Heat 16-19 of C-terminal are considered as flexible regions and they are driving away from each other, so it is logical to expect the dissociation of RanGTP during the transition. Moreover, Cook [22] pointed out that Heat 17 of Xpot may play an important role in the binding of RanGTP and Xpot. Consequentially, Xpot may not be able to bind with RanGTP based on the observation that distance between Heat 17 and regions of N-terminal arch(Heat 1-7) is getting longer during the transition (Movie S4).

On the other hand, tRNA may no longer stay in the bound state as seen from the predicted pathway. This may result from that overall shape of tRNA and Xpot are highly complementing to each other and this structural characteristic does not remain long during the predicted transition. For instance, D and TΨC loops of tRNA are located in the curved surface of C-terminal arch of Xpot [22], and then this complementary structure does not remain the same during the transition (Movie S2 to S4). Another example is that the CCA sequence at the 3' end of tRNA is located in a groove which is generated by Heat 4 and Heat 7 [22], and this groove will not remain the same, either. The above observations suggest that the geometric constraints of being able to bind Xpot and tRNA will be changed because of the flexibility of Xpot.

Normal mode analysis is a good computational technique for studying dynamics of macromolecules [11, 23–

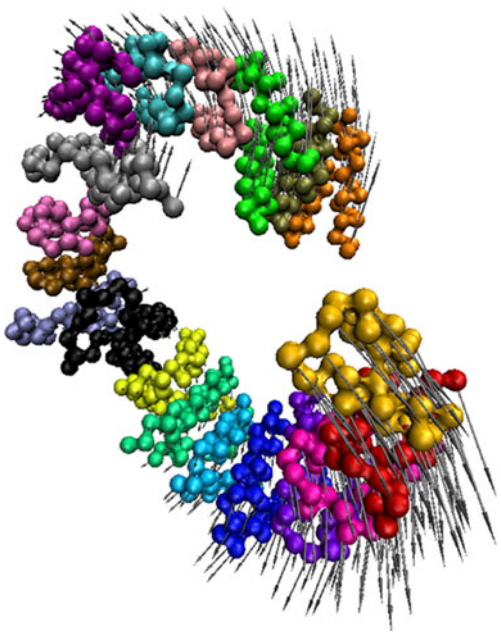

Fig. 8 The first mode of 3ICQ. Arrows are relative amplitude and the direction of alpha carbons along the obtained normal mode (eigenvector) from EN-NMA

26]. The key feature is that a macromolecule's dynamics can be described as 3 N independent normal modes (N is the number of atoms). Some studies showed that more than half out of 3800 known proteins' motions can be approximately captured by at least their two lowest normal modes [27, 28]. As a result, in addition to report the transition of Xpot regarding the conformational change, EN-NMA was conducted on the bound state of Xpot (3ICQ).

Two values, overlap and quality of motion description were calculated for interpreting the result of EN-NMA. Given a normal mode, a_j, and conformational change, $\Delta\vec{r}$, the value of overlap can be computed from Eq. 2

$$I(overlap) = \left|\vec{a}_j \cdot \Delta\vec{r}\right| = \frac{\left|\sum a_{i,j}\left(r_i^o - r_i^c\right)\right|}{\sqrt{\sum a_{i,j}^2 \sum \left(r_i^o - r_i^c\right)^2}}, \quad \Delta\vec{r} = r^o - r^c \tag{2}$$

where r_i^o and r_i^c are coordinates of the ith atom in open and closed form, respectively [29]. It calculates the cosine value between two given vectors, so it indicates how much the direction of a given normal mode is close to that of a known conformational change of a macromolecule. To examine how accurately a set of calculated normal modes describe collective motions of a macromolecule, the quality of the motion description, Q_d is used as defined in Eq. 3 [30]

$$Q_d = 100 \cdot \sum_j^{3N} I_j^2 \tag{3}$$

where I_j is the value of overlap of the jth mode. It notes that Q_d will be equal to 100% when all 3 N modes are taken into account. Roughly speaking, if the Q_d value for the first non-rigid mode is 80%, it would mean that this mode captures 80% of its conformational change in the sense of topological overlap.

The results of EN-NMA indicated that the value of overlap was 0.708 for the first mode and the first two modes could reach up to 92% of quality of motion description as shown in Fig. 7. This indicated that the first two modes were dominant to the bound state of Xpot. Moreover, Fig. 8 shows the vector representations of the relative amplitude and the direction of alpha carbons along the most dominant mode (i.e., the first mode) obtained from EN-NMA. According to Fig. 8, Heat 13-19 and Heat 1-7 have larger relative atomic displacements which is analogous to the results of ENI that Heat 1-4 of N-terminal arch and Heat 16-19 of C-terminal arch have larger displacements in terms of RMSD during the transition. The observation from the dynamic behaviors in terms of direction and magnitude of the first mode suggests that bound state of Xpot (3ICQ) not only may have the tendency to match the predicted pathway which described the cargo-induced conformational change, but also may have the ability to transport cargos because of the flexible regions of Xpot.

Conclusions

In this study, the authors constructed elastic network models of exportins (Cse1p and Xpot) to investigate their transitions of conformational changes which occur upon transport of cargos between the nucleus and cytoplasm. A series of intermediates was generated by ENI, and the results were in good agreement with Zachariae's work in two perspectives. One was that of the formation of ring closure was observed from the predicted intermediates. The other was that of the values of average RMSD during the transition which indicated the flexibility of Cse1p.

In the case of Xpot, the observed flexibility might be crucial for releasing RanGTP and tRNA during the nucleocytoplasmic transport. In the bound state of Xpot, structures of three biological components are highly complementing to each other, which result in some geometric constraints for bindings and interactions. Consequently, the flexibility of Xpot might make dissociations of tRNA and RanGTP possible during the predicted pathway (Movie S2–S4). Moreover, all Heat repeats display an interesting pattern during the pathway that there are two distinct increases of average RMSD around 20th and 50th intermediates. In addition to the predicted pathway, the results of EN-NMA on the bound state of Xpot indicated that the first two dominant modes can reach approach 92% for the quality of motion description. Furthermore, the dynamic behavior of the first mode in Xpot presented in Fig. 8 suggested that bound state of Xpot (3ICQ) may have the tendency to match the predicted pathway and the ability of transport cargos because of the observed flexible regions.

Acknowledgments The authors would like to acknowledge the precious help from Professor Moon Kim of Sungkyunkwan University in Korea, which included providing simulation codes and technical discussions of Elastic Network based Interpolation and Normal Mode Analysis.

References

1. Conti E, Izaurralde E (2001) Nucleocytoplasmic transport enters the atomic age. Curr Opin Cell Biol 13:310–319
2. Macara IG (2001) Transport into and out of the nucleus. Microbiol Mol Biol Rev 65:570–594
3. Chook YM, Blobel G (2001) Karyopherins and nuclear import. Curr Opin Struct Biol 11:703–715
4. Conti E, Muller CW, Stewart M (2006) Karyopherin flexibility in nucleocytoplasmic transport. Curr Opin Struct Biol 16:237–244
5. Görlich D, Kutay U (1999) Transport between the cell nucleus and the cytoplasm. Annu Rev Cell Dev Biol 15:607–660

6. Madrid AS, Weis K (2006) Nuclear transport is becoming crystal clear. Chromosoma 115:98–109
7. Stewart M (2007) Molecular mechanism of the nuclear protein import cycle. Nat Rev Mol Cell Biol 8:195–208
8. Cook A, Bono F, Jinek M, Conti E (2007) Structural biology of nucleocytoplasmic transport. Annu Rev Biochem 76:647–671
9. Kim MK, Chirikjian GS, Jernigan RL (2002) Elastic models of conformational transitions in macromolecules. J Mol Graph Model 21:151–160
10. Tirion MM (1996) Large amplitude elastic motions in proteins from a single-parameter atomic analysis. Phys Rev Lett 77:1905–1908
11. Bahar I, Lezon TR, Bakan A, Shrivastava IH (2010) Normal mode analysis of biomolecular structures: functional mechanisms of membrane proteins. Chem Rev 110:1463–1497
12. Hinsen K (1998) Analysis of domain motions by approximate normal mode calculations. Proteins 33:417–429
13. Bahar I, Rader AJ (2005) Coarse-grained normal mode analysis in structural biology. Curr Opin Struct Biol 15:586–592
14. Kim MK, Jernigan RL, Chirikjian GS (2003) An elastic network model of HK97 capsid maturation. J Struct Biol 143:107–117
15. Künzler M, Hurt EC (1998) Cselp functions as the nuclear export receptor for importin a in yeast. FEBS Lett 433:185–190
16. Kutay U, Bischoff FR, Kostka S, Kraft R, Görlich D (1997) Export of importin alpha from the nucleus is mediated by a specific nuclear transport factor. Cell 90:1061–1071
17. Matsuura Y, Stewart M (2004) Structural basis for the assembly of a nuclear export complex. Nature 432:872–877
18. Cook A, Fernandez E, Lindner D, Ebert J, Schlenstedt G, Conti E (2005) The structure of the nuclear export receptor Cse1 in Its cytosolic state reveals a closed conformation incompatible with cargo binding molecular. Cell 18:355–367
19. Zachariae U, Grubmuller H (2006) A highly strained nuclear conformation of the exportin Cse1p revealed by molecular dynamics simulations. Structure 14:1469–1478
20. Rodriguez MS, Dargemont C, Stutz F (2004) Nuclear export of RNA. Biol Cell 96:639–655
21. Köhler A, Hurt E (2007) Exporting RNA from the nucleus to the cytoplasm. Nat Rev Mol Cell Biol 8:761–773
22. Cook AG, Fukuhara N, Jinek M, Conti E (2009) Structures of the tRNA export factor in the nuclear and cytosolic states. Nature 461:60–66
23. Ma J (2005) Usefulness and limitations of normal mode analysis in modeling dynamics of biomolecular complexe. Structure 13:373–380
24. Cui Q, Li G, Ma J, Karplus M (2004) A normal mode analysis of structural plasticity in the biomolecular motor F1-ATPase. J Mol Biol 340:345–372
25. Brooks B, Karplus M (1983) Harmonic dynamics of proteins: normal modes and fluctuations in bovine pancreatic trypsin inhibitor. Proc Nat Acad Sci USA 80:6571–6575
26. Tama F, Brook CL (2006) Symmetry form and shape: guiding principles for robustness in macromolecular machines. Annu Rev Biophys Biomol Struct 35:115–133
27. Suhre K, Sanejouand YH (2004) ElNémo: a normal mode web server for protein movement analysis and the generation of templates for molecular replacement. Nucl Acid Res 32:W610–W614
28. Krebs WG, Alexandrov V, Wilson CA, Echols N, Yu H, Gerstein M (2002) Normal mode analysis of macromolecular motions in a database framework: developing mode concentration as a useful classifying statistic. Proteins Struct Funct Bioinf 48:682-695
29. Tama F, Gadea FX, Marques O, Sanejouand YH (2000) Building-block approach for determining low-frequency normal modes of macromolecules. Proteins Struct Funct Bioinf 41:1–7
30. Nicolay S, Sanejouand YH (2006) Functional modes of proteins are among the most robust. Phys Rev Lett 96:078101–078104
31. Humphrey W, Dalke A, Schulten K (1996) VMD - visual molecular dynamics. J Mol Graph 14:33–38